

ChemComm

Accepted Manuscript



This is an *Accepted Manuscript*, which has been through the RSC Publishing peer review process and has been accepted for publication.

Accepted Manuscripts are published online shortly after acceptance, which is prior to technical editing, formatting and proof reading. This free service from RSC Publishing allows authors to make their results available to the community, in citable form, before publication of the edited article. This *Accepted Manuscript* will be replaced by the edited and formatted *Advance Article* as soon as this is available.

To cite this manuscript please use its permanent Digital Object Identifier (DOI®), which is identical for all formats of publication.

More information about *Accepted Manuscripts* can be found in the [Information for Authors](#).

Please note that technical editing may introduce minor changes to the text and/or graphics contained in the manuscript submitted by the author(s) which may alter content, and that the standard [Terms & Conditions](#) and the [ethical guidelines](#) that apply to the journal are still applicable. In no event shall the RSC be held responsible for any errors or omissions in these *Accepted Manuscript* manuscripts or any consequences arising from the use of any information contained in them.

Cite this: DOI: 10.1039/c0xx00000x

www.rsc.org/xxxxxx

ARTICLE TYPE

Excellent Chirality Transcription in Two-Component Photochromic Organogels Assembled through *J*-Aggregation

Suman K. Samanta,^a Santanu Bhattacharya^{*a,b}

Received (in XXX, XXX) Xth XXXXXXXXXX 20XX, Accepted Xth XXXXXXXXXX 20XX

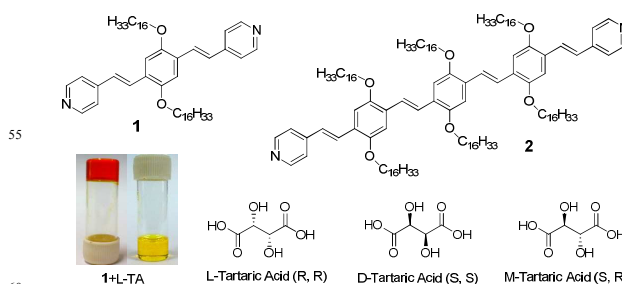
DOI: 10.1039/b000000x

Organogels made of pyridine-end oligo-*p*-phenylenevinylenes with tartaric acid exhibit remarkable *J*-aggregation induced red-shifts ($\Delta\lambda = 55$ nm) and notable chirality transcription. Induction of liquid-crystalline behavior is also tuned in the supramolecular assembly.

Supramolecular organization to a well-defined architecture may occur by selective association of complementary components through molecular recognition.¹ The information stored in the individual components are expressed in the assembly. Development of chiral supramolecular assemblies from achiral monomers through transcription of chirality have attracted much attention in mimicking the biological helical structures, liquid crystals, physical gels and recently the synthesis of self-assembled one-dimensional stacks.² Supramolecular gelation via molecular recognition in a specific solvent or solvent mixtures could be a vehicle for generating such chiral nanomaterials³ as a consequence of various non-covalent interactions.⁴ Specifically, π -stacking interactions play a major role in the gelation of conjugated chromophoric molecules, where the chromogenic part offers an extra handle to probe their aggregation-induced changes in the optoelectronic properties.⁵ In particular, Park *et al.* reported gelation-induced enhanced emission and chirality transcription in the H-bonded tartaric acid (TA) with a pyridine based non-fluorescent molecule.⁶ However, controlled organization of such molecules dictated by another component to generate specific and predictable chiral nano-structures still remains a challenge. Herein, we report organogelation of new chromophoric pyridine-end oligo-*p*-phenylenevinylenes (OPV, **1** and **2**, Scheme 1) in assistance with isomeric TAs *viz.* L-tartaric acid (L-TA) and D-tartaric acid (D-TA) as well as chirality transcription in the supramolecular assembly via *J*-aggregate formation. Also, thermal mesophases of the complexes could be tuned depending on the TA isomers used.

Pre-gelators **1** and **2** were synthesized using Wittig reaction and were characterized unambiguously (Scheme S1, ESI†). TA complexes of **1** and **2** in 1:1 molar ratio were prepared and tested for gelation. It was observed that none of the complexes were soluble in non-polar solvents like toluene or *n*-heptane. Although soluble in polar solvents like ethanol or THF they did not form gel either. However, gelation was observed in a mixture of toluene and ethanol at a particular ratio (10:1 v/v respectively). With less amount of ethanol in the mixture, the complexes could not be solubilized properly while it remained as a solution with

excess ethanol, indicating a crucial hydrophilic/hydrophobic balance is operational for the self-assembly that leads to gelation.



Scheme 1 The pre-gelators **1** and **2** and three different TA used here for the gelation studies. Snapshot of a typical gel and sol of **1**+L-TA in 10:1 toluene/ethanol (v/v) mixture.

Although, gelation occurred with **1**+L-TA and **1**+D-TA complexes with a minimum gelator concentration (MGC) of 0.93 and 1.1 wt% respectively in 10:1 toluene/ethanol mixture, **1**+M-TA (meso-tartaric acid) did not form gel at all. This suggests that the spatial orientation of the -COOH moiety in the chiral TA holds the key to favor the mode of aggregation that is conducive for gel formation.⁶ Thus, a 1:1 mixture of **1**+L-TA and **1**+D-TA (above individual MGCs) did not form gel probably due to the inter-gelator interactions. However, the gelation was observed in each of the complexes (1:1) of **2** with L-TA, D-TA and M-TA having MGC 0.87, 0.92 and 1.14 wt% respectively presumably due to the enhanced π -stacking and van der Waals interactions through the five aromatic rings and six *n*-hexadecyl chains of **2** respectively. In contrast, **1** and **2** alone failed to form a gel. Presence of hydroxyl groups on the TA moiety is also crucial, as the gelation did not occur when tested with mixtures of **1** with either oxalic or succinic acid. Protonation of the pyridine-ends of **1** and **2** by TA was evident from the IR stretching frequency of the free -COOH (1730 cm^{-1}) which decreased to 1612 cm^{-1} upon complexation with **1** or **2** indicating formation of -COO⁻ species (Fig. S1†). Each gel was optically transparent (Fig. S2†) and a typical gel *e.g.* **1**+L-TA displayed a red color at 25 °C while it transformed into a yellow sol when heated to 60 °C (Scheme 1).

Morphological analysis of the complexes using transmission electron microscopy revealed the presence of fibrillar networks with diameter ~200-300 nm. With increasing concentration, a nucleation induced aggregated structures were observed under the fluorescence and scanning electron microscopy (Fig. S3-S5†).

Circular dichroism (CD) spectral studies verified the chiral transcription abilities of the self-assembly of the isomeric TAs with each of the pre-gelators **1** and **2**. A uniform cast film of the layered gels of **1**+TA revealed a bisignated Cotton effect producing a strong CD signal close to 500 nm with zero crossings at 366 and 293 nm (Fig. 1). This leads to virtually mirror image spectra for the complexes with two enantiomers (L- and D-TA) indicating the transfer of chiral information of TA to the self-assembled chromophores in a helical sense.¹ Similar mirror-image spectra were observed in the CD signals of the **2**+TA complexes showing a strong band at 520 nm with zero crossings at 610, 466 and 265 nm. The D-TA complexes showed a peak first followed by a trough which indicates a right-handed helical assembly (P) and conversely a left-handed helical assembly (M) for L-TA complexes was indicated.⁷ However, the complexes containing M-TA for both **1** and **2** showed no helical bias.

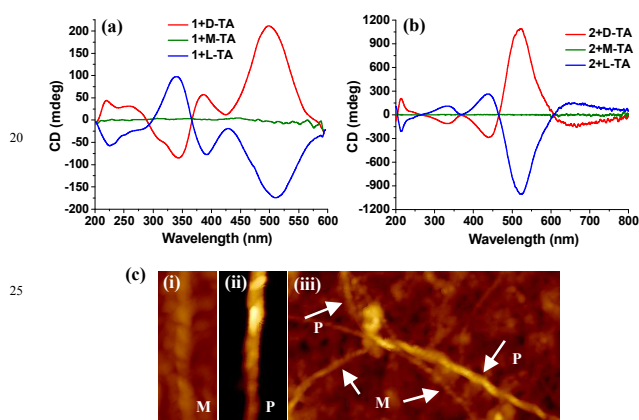


Fig. 1 Circular dichroism spectra of (a) **1**+TA and (b) **2**+TA complexes. (c) AFM topographic images showing (i) M-helix for **1**+L-TA, (ii) P-helix for **1**+D-TA and (iii) mixture of M and P-helices for **1**+M-TA.

Under an atomic force microscope, 'rope'-like M-helical fibers from **1**+L-TA and P-helices from **1**+D-TA were clearly visible with high aspect ratios (Fig. 1 and S6†). The fiber diameters ranged within 200-300 nm. Interestingly, **1**+M-TA showed presence of both P and M helices together, a resultant of which averaged out in the CD spectra. The helix formation in the achiral components of **1**+M-TA could be a consequence of supramolecular self-assembly with no preferable handedness. In addition to the fibrillar morphologies, it also furnished ring-like assemblies of average diameter of ~500 nm. The complexes of **2**+L-TA and **2**+D-TA showed M and P type helical fibers respectively with the average fiber diameters of 100-150 nm. Thus, the information stored in the individual TA components was expressed specifically in the assembly through chirality transcription, a phenomenon of particular interest.^{6,8}

Photophysical studies of **1** (10 μ M) in 10:1 toluene/ethanol mixture showed absorption maxima at 400 and 330 nm and an emission maximum at 468 nm (λ_{ex} 380 nm, Fig. S7†). Corresponding absorption and emission maximum of **2** appeared at higher wavelengths at 456 and 525 nm respectively (λ_{ex} 450 nm) due to a greater conjugation length in **2**. The excitation spectra of both **1** and **2** are consistent with their respective absorption spectra (Fig. S8†). A higher quantum yield of **1** (0.78) over **2** (0.50) indicates a favorable non-radiative fluorescence

decay of **1**. Both **1** and **2** showed solvatochromic effect and the solvent-induced shifts were greater in the emission maximum than in the absorption maximum indicating that the excited states are more sensitive towards the solvent polarity (Fig. S9†). Thus, by changing the polarity of the solvent from *n*-heptane to chloroform, the emission maximum shifted from 442 nm to 465 nm ($\Delta\lambda = 23$ nm) for **1** and 506 nm to 527 nm ($\Delta\lambda = 21$ nm) for **2**.

Interestingly, in the gel phase, the emission spectra showed remarkable red-shifts. The emission maximum of a gel of **1**+L-TA appeared at 575 nm (λ_{ex} 380 nm) and for **2**+L-TA it was 660 nm (λ_{ex} 540 nm) at 25 °C (Fig. S10†). Corresponding emission maximum of the 'sol' at 60 °C appeared at 520 nm and 625 nm respectively. Variable temperature fluorescence spectral studies (Fig. 2) showed gradual hypochromic red-shifts in the emission maximum from 520 nm to 575 nm ($\Delta\lambda = 55$ nm) for **1**+L-TA and 625 nm to 660 nm ($\Delta\lambda = 35$ nm) for **2**+L-TA respectively on transformation from sol-to-gel indicating a J-type of aggregate formation (Fig. S11†).⁹ A plot of the intensity at the emission maximum vs. temperature produces a sigmoidal curve showing a sol-to-gel transition temperature at ~40 °C at this concentration (1.15 wt% for both, Fig. S12†). The gels under a 365 nm UV-lamp showed a light-red emission for **1**+L-TA and a red emission for **2**+L-TA (Fig. 2 and S2†). However, the sol at 60 °C showed a bright yellow emission for **1**+L-TA while a bright orange emission for **2**+L-TA.

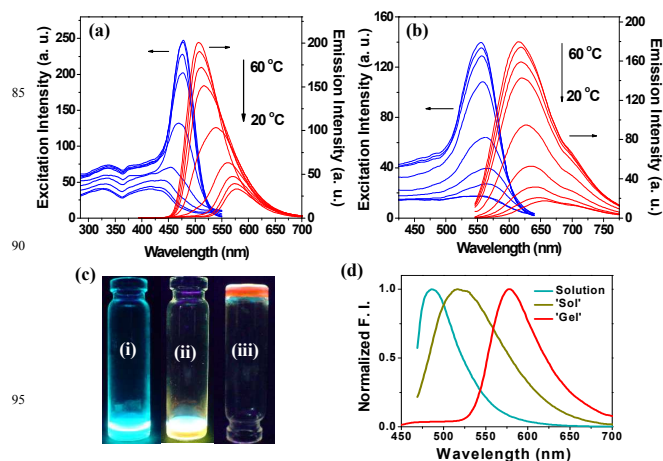


Fig. 2 Variable temperature excitation and emission spectra of (a) **1**+L-TA (λ_{ex} 380 nm, λ_{em} 575) and (b) **2**+L-TA (λ_{ex} 470 nm, λ_{em} 660). (c) Snapshots showing (i) **1** as solution, (ii) **1**+L-TA as 'sol' at 60 °C, (iii) **1**+L-TA as gel at 25 °C and (d) corresponding emission spectra. Concentration 1.15 wt% in 10:1 toluene/ethanol mixture in each case.

However, this type of spectral shift on temperature variation was not observed for the solution of **1** alone at an identical concentration (1.15 wt%, Fig. S10c†). It showed an emission maximum at 482 nm which corresponds to a bright sky-blue emission (Fig. 2c). The emission color changed to bright yellow in the 'sol' of **1**+L-TA at 60 °C leading to a red-shifted emission band at 520 nm (Fig. 2d). Finally the emission color changed to light-red in the gel at 25 °C showing an emission maximum at 575 nm. Therefore, these emission changes and the remarkable red-shifts occur as a consequence of two consecutive phenomena: (i) protonation of the pyridine N by TA leading to a shift from 482 to 520 nm ($\Delta\lambda = 38$ nm) and (ii) J-aggregation induces a

further shift in the emission maximum from 520 to 575 nm ($\Delta\lambda = 55$ nm). Theoretical calculations were undertaken to explain the effect of protonation on the red-shifts in the emission spectra (Fig S13, S14[†]). It showed that upon protonation, the HOMO and LUMO energy gap decreases significantly which accounts for a higher emission λ_{max} (Table S1[†]). It may be further noted that the systems attain planarity on protonation and these planar aromatic surfaces may offer effective π -stacking interactions leading to excellent *J*-aggregation.

Presence of thermotropic mesophases in the pre-gelators and in complexes were investigated using differential scanning calorimetry and polarized optical microscopy (POM). Compound **1** alone showed a sharp phase-transition at 111.3 °C for melting and at 102.3 °C for freezing (Fig. S15[†]). The phase-transition temperature of **1**+TA showed a decrease of ~ 7 °C for the heating cycle and ~ 11 °C for the cooling cycle (Table S2[†]). Similar extent of decrease in the phase transition temperature was also observed for **2**+TA complexes than **2** alone indicating a change in the supramolecular organization¹⁰ in the TA complexes.

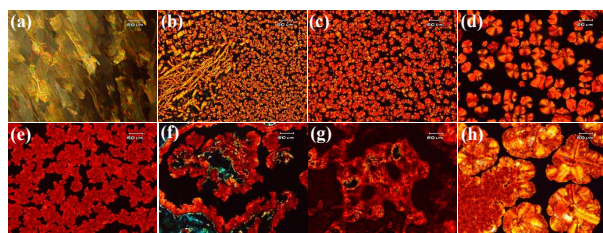


Fig. 3 POM images of (a) **1**, (b) **1**+L-TA, (c) **1**+D-TA, (d) **1**+M-TA and (e) **2**, (f) **2**+L-TA, (g) **2**+D-TA, (h) **2**+M-TA.

POM images showed birefringent textures from **1**, **2** and their TA complexes which were monitored by taking snapshots upon progressively decreasing temperature of the isotropic melts (Fig. 3, S16-S19[†]). In case of **1**, only a crystalline phase appeared all at once at ~ 107 °C while for **1**+L-TA, initially a rod-like texture appeared at 120 °C followed by another type of smaller domain of distinct morphology at ~ 110 °C and finally a crystalline phase appeared rapidly at ~ 83 °C. However, **1**+D-TA showed only the smaller domain morphology followed by a crystalline phase. Interestingly, **1**+M-TA revealed focal-conic morphology possibly due to the formation of smectic phase along with smaller domains.¹¹ The birefringent textures were liquid-crystalline in nature before appearing the rapidly growing phase starting at ~ 83 °C for **1**+L-TA, ~ 90 °C for **1**+D-TA and ~ 85 °C for **1**+M-TA complexes. These observations suggest that the appearance of smaller domains are predominantly due to the helical fibers (for **1**+L-TA and **1**+D-TA) while the focal-conic morphology is possibly due to the ring-like structures of **1**+M-TA. Interestingly, an opposite phenomena appeared in case of **2** which showed liquid-crystalline behavior upto ~ 130 °C while none of the complexes of TAs with **2** showed any liquid-crystalline behavior, rather they all showed crystalline phases. Thus the birefringent textures are dictated by the spatial orientations of TA isomers.

In conclusion, it is shown for the first time, that pyridine-end OPVs form supramolecular organogels via molecular recognition of the chiral forms of TA. The chiral information stored in TA induces exactly opposite sense of chirality in the complexes for two optically active TA (L- and D-). This leads to the formation

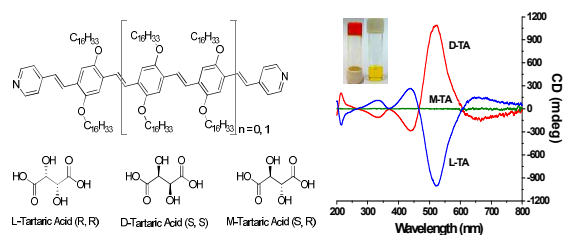
of P- and M-helical fibers for the complexes containing D-TA and L-TA respectively while both helices exist in the complexes derived from M-TA. Notable red-shifts in the emission maxima are observed as a consequence of protonation and *J*-aggregation induced gel formation. Thermal mesophases could also be tuned depending on the spatial orientation of different TA isomers. Such tunable systems deserve further research for the generation of specific and predictable chiral supramolecular stacks through chiral induction.

S.B. thanks J.C. Bose Fellowship (DST) for funding this work.

Notes and references

- ^a Department of Organic Chemistry, Indian Institute of Science, Bangalore-560012, India. Fax: +91-80-23600529; Tel: +91-80-22932664; E-mail: sb@orgchem.iisc.ernet.in
- ^b Chemical Biology Unit, Jawaharlal Nehru Centre for Advanced Scientific Research, Bangalore-560064, India.
- [†] Electronic Supplementary Information (ESI) available: Experimental section, synthesis and supporting figures (S1-S19). See DOI: 10.1039/b000000x/
- J.-M. Lehn, *Angew. Chem. Int. Ed. Engl.*, 1990, **29**, 1304; T. Gulic-Krzywicki, C. Fouquey, J.-M. Lehn, *Proc. Natl. Acad. Sci. USA*, 1993, **90**, 163; R. Oda, I. Huc, M. Schmutz, S. J. Candau, F. C. MacKintosh, *Nature*, 1999, **399**, 566; C. C. Lee, C. Grenier, E. W. Meijer, A. P. H. J. Schenning, *Chem. Soc. Rev.*, 2009, **38**, 671; S. J. George, Z. Tomovic, A. P. H. J. Schenning, E. W. Meijer, *Chem. Commun.*, 2011, **47**, 3451.
 - S. J. George, R. de Bruijn, Z. Tomovic, B. V. Averbek, D. Beljonne, R. Lazzaroni, A. P. H. J. Schenning, E. W. Meijer, *J. Am. Chem. Soc.*, 2012, **134**, 17789; H. Nakade, B. J. Jordan, S. Srivastava, H. Xu, X. Yu, M. A. Pollier, G. Cooke, V. M. Rotello, *Supramol. Chem.*, 2010, **22**, 691; R. Oda, F. Artzner, M. Laguerre, I. Huc, *J. Am. Chem. Soc.*, 2008, **130**, 14705; J. J. D. de Jong, L. N. Lucas, R. M. Kellogg, J. H. van Esch, B. L. Feringa, *Science*, 2004, **304**, 278; R. Custelcean, M. D. Ward, *Angew. Chem., Int. Ed.*, 2002, **41**, 1724.
 - B. Adhikari, J. Nanda, A. Banerjee, *Soft Matter*, 2011, **7**, 8913; X. Zhu, P. Duan, L. Zhang, M. Liu, *Chem. Eur. J.* 2011, **17**, 3429-3437; S. K. Batabyal, W. L. Leong, J. J. Vittal, *Langmuir*, 2010, **26**, 7464; C. Bao, R. Lu, M. Jin, P. Xue, C. Tan, G. Liu, Y. Zhao, *Org. Biomol. Chem.*, 2005, **3**, 2508.
 - S. Bhattacharya, S. K. Samanta, *Langmuir*, 2009, **25**, 8378; M. George, R. G. Weiss, *Acc. Chem. Res.*, 2006, **39**, 489; S. Bhattacharya, S. K. Samanta, *Chem. Eur. J.*, 2012, **18**, 16632.
 - S.-J. Yoon, J. H. Kim, J. W. Chung, S. Y. Park, *J. Mater. Chem.*, 2011, **21**, 18971; S. K. Samanta, A. Pal, S. Bhattacharya, *Langmuir*, 2009, **25**, 8567; J. F. Hulvat, M. Sofos, K. Tajima, S. I. Stupp, *J. Am. Chem. Soc.*, 2005, **127**, 366; S. K. Samanta, S. Bhattacharya, *J. Mater. Chem.*, 2012, **22**, 25277.
 - J. Seo, J. W. Chung, E.-H. Jo, S. Y. Park, *Chem. Commun.*, 2008, 2794.
 - S. J. George, A. Ajayaghosh, P. Jonkheijm, A. P. H. J. Schenning, E. W. Meijer, *Angew. Chem. Int. Ed.* 2004, **43**, 3422.
 - S. J. George, Z. Tomovic, M. M. J. Smulders, T. F. A. de Greef, P. E. L. G. Leclere, E. W. Meijer, A. P. H. J. Schenning, *Angew. Chem. Int. Ed.* 2007, **46**, 8206; R. Amemiya, M. Mizutani, M. Yamaguchi, *Angew. Chem. Int. Ed.*, 2010, **49**, 1995; M. R. Molla, A. Das, S. Ghosh, *Chem. Commun.*, 2011, **47**, 8934.
 - F. Wurthner, T. E. Kaiser, C. R. Saha-Moller, *Angew. Chem. Int. Ed.*, 2011, **50**, 3376; H. Wu, L. Xue, Y. Shi, Y. Chen, X. Li, *Langmuir*, 2011, **27**, 3074.
 - S. K. Samanta, A. Pal, S. Bhattacharya, C. N. R. Rao, *J. Mater. Chem.*, 2010, **20**, 6881; S. K. Samanta, K. S. Subrahmanyam, S. Bhattacharya, C. N. R. Rao, *Chem. Eur. J.* 2012, **18**, 2890.
 - V. N. Vijayakumar, K. Murugadass, M. L. N. Madhu Mohan, *Mol. Cryst. Liq. Cryst.*, 2010, **517**, 43.

Graphical Abstract

Excellent Chirality Transcription in Two-Component Photochromic Organogels Assembled through *J*-AggregationSuman K. Samanta,^a Santanu Bhattacharya^{*a,b}^aDepartment of Organic Chemistry, Indian Institute of Science, Bangalore-560012, India.
Fax: +91-80-23600529; Tel: +91-80-22932664; E-mail: sb@orgchem.iisc.ernet.in^bChemical Biology Unit, Jawaharlal Nehru Centre for Advanced Scientific Research, Bangalore-560064, India.

Gelation of optically-active tartaric acid and pyridine-end oligo-phenylenevinylens brings about selective chirality transcription, fluorescence modulation and formation of altered mesophases.